

lined above using finite-range form factors with DWUCK. The shapes of the angular distributions are nearly the same as those obtained from no-recoil calculations. The relative spectroscopic factors extracted are listed in Table I together with the L transfer and the L_R used to calculate the recoil correction terms. The effect of the recoil corrections is to reduce significantly the differences in the spectroscopic factors for the j_z and j_y states in both the ^{12}C - and ^{16}O -induced reactions. While there are still problems, such as the predicted energy dependence of the (^{16}O , ^{15}N) transfers to the j_y states, the agreement with the light-ion results is much improved. Even better agreement is probably hindered by the approximations made in the present treatment. Most serious is our approximation for the overlap integral, which is valid only for weakly bound states.⁶ Nevertheless, the results demonstrate that the largest part of the discrepancies can be removed by including recoil effects.

We conclude from our study that recoil effects in heavy-ion transfer reactions can be large and that they must be treated properly before spectroscopic information can be extracted reliably.

*Work performed under the auspices of the U. S. Atomic Energy Commission.

†On leave from Hahn-Meitner Institut, Berlin, Ger-

many.

‡On leave from Max-Planck-Institut für Kernphysik, Heidelberg, Germany.

¹See, e.g., *Nuclear Reactions Induced by Heavy Ions*, edited by R. Bock and W. Hering (North-Holland, Amsterdam, 1970); *J. Phys. (Paris)* **32**, Suppl. 11-12 (1971); *J. Phys. (Paris)* **33**, Suppl. 8-9 (1972).

²R. D. Becchetti, P. R. Christensen, V. I. Manko, and R. J. Nickles, *Phys. Lett.* **43B**, 279 (1973).

³K. R. Greider, in *Nuclear Reactions Induced by Heavy Ions*, edited by R. Bock and W. Hering (North-Holland, Amsterdam, 1970).

⁴P. J. A. Buttle and L. J. B. Goldfarb, *Nucl. Phys.* **78**, 409 (1966), and **A176**, 299 (1971).

⁵R. M. DeVries and K. I. Kubo, *Phys. Rev. Lett.* **30**, 325 (1973).

⁶M. A. Nagarajan, *Nucl. Phys.* **A196**, 34 (1972).

⁷B. G. Harvey, J. Mahoney, F. G. Pühlhofer, F. S. Golding, D. A. Landis, J.-C. Faivre, D. G. Kovar, M. S. Zisman, J. R. Meriwether, S. W. Cospers, and D. L. Hendrie, *Nucl. Instrum. Methods* **104**, 21 (1972).

⁸D. G. Kovar, F. D. Becchetti, B. G. Harvey, F. G. Pühlhofer, J. Mahoney, D. W. Miller, and M. S. Zisman, *Phys. Rev. Lett.* **29**, 1023 (1972).

⁹F. Schmittroth, W. Tobocman, and A. Golestaneh, *Phys. Rev. C* **1**, 377 (1970).

¹⁰W. Tobocman, private communication.

¹¹P. D. Kunz, private communication.

¹²J. C. Hiebert, E. Newman, and R. H. Bassel, *Phys. Rev.* **154**, 898 (1967); A. R. Barnett, W. R. Phillips, P. J. A. Buttle, and L. J. B. Goldfarb, *Nucl. Phys.* **A176**, 321 (1971).

¹³M. S. Zisman *et al.*, Lawrence Berkeley Laboratory Report No. LBL 1676, 1972 (to be published).

Anomalous and Normal Angular Distributions in Ni(^{18}O , ^{16}O) Reactions*

E. H. Auerbach, A. J. Baltz, P. D. Bond, C. Chasman, J. D. Garrett, K. W. Jones, S. Kahana, M. J. LeVine, M. Schneider, A. Z. Schwarzschild, and C. E. Thorn

Brookhaven National Laboratory, Upton, New York 11973

(Received 22 February 1973)

Differential cross sections are measured for $^{58,60,62,64}\text{Ni}(^{18}\text{O}, ^{16}\text{O})$ reactions to both ground and excited (2^+) states of the residual Ni nuclei at incident ^{18}O laboratory energies of 65, 57, and 50 MeV. Anomalous, forward-rising, angular distributions are seen for $^{58,60}\text{Ni}(^{18}\text{O}, ^{16}\text{O})$ reactions, in contrast to normal heavy-ion-induced transfer shapes obtained for the heavier Ni targets. A theoretical explanation is presented based on a weaker absorption than is usually employed for such heavy-ion transfer reactions.

It has been generally accepted¹ that few-nucleon transfer between heavy-ion projectiles and reasonably massive target nuclei can be described in a strongly absorbing, semiclassical model. The transfer is confined to the periphery of the interacting nuclei where the strong Coulomb field between the ions is dominant. The projec-

tile is imagined to travel along a well-defined orbit in this exterior region and the transfer takes place from a trajectory matched smoothly between entrance and exit channels. The result should be a cross section which is optimum for Q values and angles corresponding to a favored, grazing collision. Such cross sections have been

observed in angular distributions^{2,3} and excitation functions⁴ of heavy-ion reactions induced on heavy and medium-heavy nuclei and have been described by distorted-wave Born-approximation (DWBA) calculations.^{5,6} This Letter presents experimental evidence for significant deviations from the characteristic shape in the angular distributions of the $^{58,60}\text{Ni}(^{18}\text{O}, ^{16}\text{O})$ transitions to the ground and first excited states of $^{60,62}\text{Ni}$. These cross sections continue rising towards the most forward angles observed. On the other hand, our angular distributions for the $^{62,64}\text{Ni}(^{18}\text{O}, ^{16}\text{O})$ reactions more closely resemble the bell-shaped curves expected from classical considerations and seen in earlier work. The anomalous $^{58,60}\text{Ni}(^{18}\text{O}, ^{16}\text{O})$ and normal $^{62,64}\text{Ni}(^{18}\text{O}, ^{16}\text{O})$ angular distributions persist over a range of incident energy.

The $(^{18}\text{O}, ^{16}\text{O})$ reaction and the ^{16}O and ^{18}O elastic scattering on even-mass Ni targets were studied using the ^{16}O and ^{18}O beams of the Brookhaven tandem Van de Graaff facility. The reaction products were detected simultaneously in an array of three ΔE - E silicon surface-barrier detector telescopes with ΔE detectors ranging from 10 to 30 μm thick. The masses of the reaction products were identified using standard particle-identifier techniques. The positive Q values of the $(^{18}\text{O}, ^{16}\text{O})$ reactions to low-lying levels in the final nucleus minimized problems with the feed-through of elastic ^{18}O events into ^{16}O spectra in the excitation region of interest. An experimental resolution typically of 250 keV [full width at half-maximum (FWHM)] was obtained with self-supporting Ni targets isotopically enriched to >98% and of $\sim 150 \mu\text{g}/\text{cm}^2$ areal density. An absolute cross-section scale accurate to $\pm 5\%$ was established for the $(^{18}\text{O}, ^{16}\text{O})$ data by normalizing to the ^{18}O elastic scattering, assumed Rutherford at forward angles. The particle identification spectra exhibited mass resolution of considerably less than 2 units (FWHM) for oxygen. Possible confusion between the $(^{18}\text{O}, ^{16}\text{O})$ reaction and other reactions is precluded in all cases by consideration of kinematic tracking and mass identification.

Angular distributions for the $\text{Ni}(^{18}\text{O}, ^{16}\text{O})$ transitions to the ground states are shown in Fig. 1. For the $^{62,64}\text{Ni}(^{18}\text{O}, ^{16}\text{O})$ transitions the differential cross section is observed to peak at a specific center-of-mass angle which systematically decreases with increasing incident energy. Angular distributions of this shape are typical of earlier heavy-ion-induced few-nucleon transfer reac-

tions.²⁻⁴ In particular the systematics of the $^{62,64}\text{Ni}(^{18}\text{O}, ^{16}\text{O})$ reactions are consistent with those observed for similar transfer reactions on a series of Mo isotopes,³ for which the Q values spanned a range comparable to that seen here.

The angular distributions (see Fig. 1) for the $(^{18}\text{O}, ^{16}\text{O})$ ground-state transitions on $^{58,60}\text{Ni}$ are, however, strikingly different in shape from those for the above transfer reactions or for the other heavy-ion-induced transfer²⁻⁴ on intermediate mass targets. The shapes in the lighter Ni isotopes are rising towards forward angles with a shoulder appearing at the angles preferred by grazing collisions.

When a strong imaginary potential ~ 40 MeV is used in a DWBA calculation, the large changes

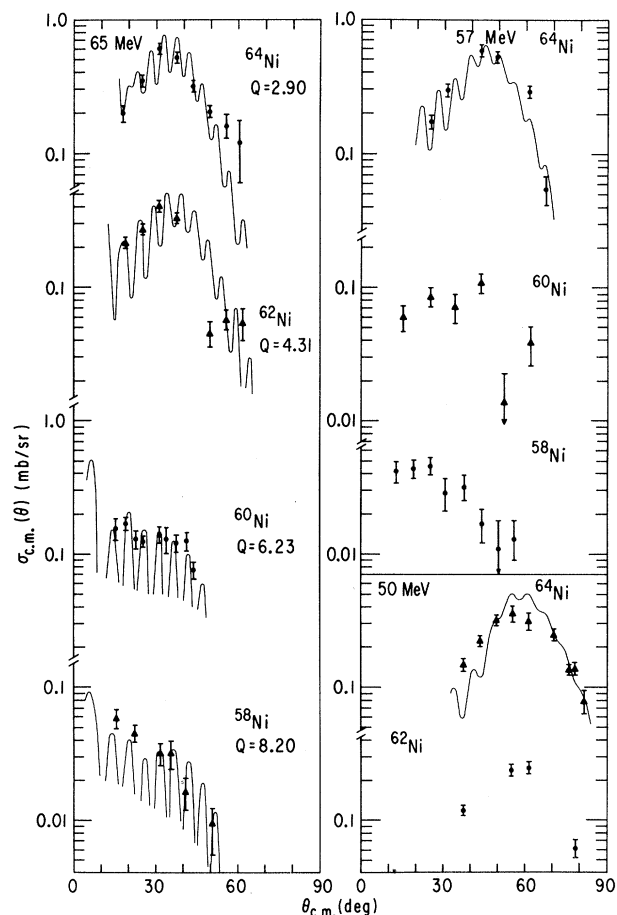


FIG. 1. Experimental differential cross sections and theoretical fits for the $^{58,60,62,64}\text{Ni}(^{18}\text{O}, ^{16}\text{O})$ ground-state transitions at incident laboratory energies of 65, 57, and 50 MeV. The DWBA curves, though containing oscillations, reproduce the change in shape from an apparently single-peaked angular distribution for the $^{62,64}\text{Ni}$ targets to the forward-sloped distribution for the $^{58,60}\text{Ni}$ targets.

in angular distribution between the reactions on $^{62,64}\text{Ni}$ and $^{58,60}\text{Ni}$ targets cannot be accounted for by the kinematic differences (Q dependence). In such a calculation, grazing angular distributions result for all of the reactions, with a slight angular shift $\lesssim 3^\circ$ evident across the Ni isotopes. One possible means of obtaining a reasonable theoretical description of the angular distributions and cross-section size is to reduce the absorption to a critically weak level which permits the heaviest Ni isotopes to be considered "strong" absorbers, but which when lowered slightly more for the lighter isotopes allows reactions to occur appreciably for angles far forward of the characteristic grazing angle. If one were to describe the elastic scattering by optical potentials with a fixed real depth and with equal real and imaginary radii, then most of the relative weakening between isotopes comes naturally from a radius decrease demanded by the (elastic) data. In this note a preliminary theoretical analysis is attempted for the $^{58,60,62,64}\text{Ni}(^{18}\text{O}, ^{16}\text{O})$ ground-state transitions at 65 MeV incident laboratory energy. This analysis employed a version of the heavy-ion finite-range DWBA code DRC,⁶ adapted for use in two-nucleon transfer reactions and previously applied to ($^{18}\text{O}, ^{16}\text{O}$) reactions in Mo isotopes.⁷ In all calculations of the transfer cross section we used *only* optical potentials fitted to the elastic scattering data. Elastic differential cross sections were measured in all entrance and exit channels (except ^{16}O on ^{66}Ni) at laboratory energies between 60 and 64 MeV. The theoretical elastic angular distributions were calculated with a heavy-ion variant of the code ABACUS and a sample fit is shown in Fig. 2. Additional fits to elastic measurements for 50-MeV-lab-energy projectiles showed no need for strong energy dependence in the optical potentials. As in earlier work,⁸ we find the elastic scattering is sensitive only to the outer region of the nuclear real potential provided a "sufficiently" strong absorption is present. There remains, however, considerable latitude in the choice of depth, range, and diffusivity for the imaginary potential. For the $^{62,64}\text{Ni}(^{18}\text{O}, ^{16}\text{O})$ reactions the optical parameters used were $V_R = 70$ MeV, $W = 9$ MeV, $a_R = a_W = 0.4$ fm, with $R_{\text{real}} = R_{\text{imag}} = 8.68$ fm and $R_{\text{real}} = R_{\text{imag}} = 8.93$ fm for ^{18}O on ^{62}Ni and ^{64}Ni , respectively, while $R_{\text{real}} = R_{\text{imag}} = 8.71$ fm and $R_{\text{real}} = R_{\text{imag}} = 8.77$ fm for ^{16}O on ^{64}Ni and ^{66}Ni , respectively. In the analysis of the $^{58,60}\text{Ni}(^{18}\text{O}, ^{16}\text{O})$ reactions, the imaginary potential depth was reduced to 8.0 MeV and the imaginary

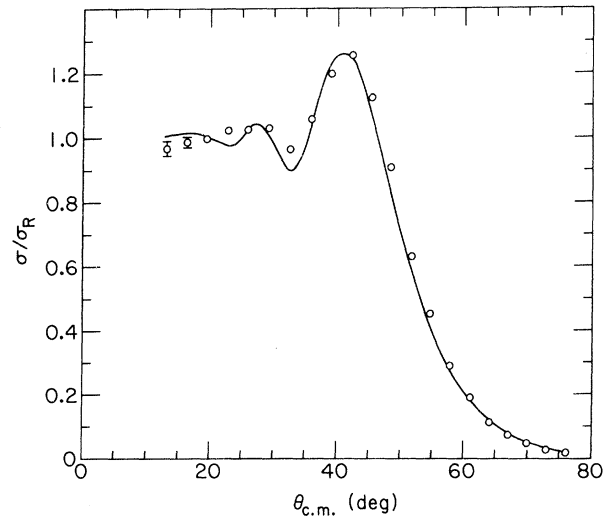


FIG. 2. Representative elastic differential cross section and fit for ^{18}O and ^{58}Ni at a laboratory energy of 63.42 MeV. Measurements were made of elastic scattering for 60–64 MeV ^{18}O and ^{16}O on the other Ni targets with almost equivalent fits obtained.

diffusivity set at 0.5 fm, while the real radii were decreased to 8.52, 8.68 fm for ^{18}O on $^{58,60}\text{Ni}$ and to 8.36, 8.31 fm for ^{16}O on $^{60,62}\text{Ni}$. Also the imaginary radii were decreased below the real values to 8.2 fm. It should again be stressed that all these parameter "changes" between the heavier and lighter isotopes are consistent with good fits to the elastic data, the change in real radii being, in fact, required by these data.

Aside from the apparent strong oscillations (Fig. 1) a reasonable grazing shape is obtained for the $^{62,64}\text{Ni}(^{18}\text{O}, ^{16}\text{O})$ angular distributions at 65 MeV. Also presented are theoretical angular distributions for the $^{64}\text{Ni}(^{18}\text{O}, ^{16}\text{O})$ reactions at incident energies of 50 and 57 MeV to illustrate our ability to describe the excitation systematics. The theoretical curves for the $^{58,60}\text{Ni}(^{18}\text{O}, ^{16}\text{O})$ ground-state transitions (Fig. 1) possess the required forward peaking but again contain strong, unobserved, oscillations. The general change in shape of angular distribution from ^{64}Ni to ^{58}Ni targets is qualitatively described in our calculations. The forward peaking is produced by transfer from orbits involving smaller nuclear separation than is experienced on grazing trajectory. Along such surface-penetrating orbits the projectile is subjected to a strong attractive nuclear field and may be bent into forward angles. The possibility of interference between several widely separated orbits has, in fact, led to the narrow angular oscillations seen in the theory, at least in our calculations based on a "no recoil"

code. There is evidence⁹ that a more exact treatment of the DWBA might considerably dampen the oscillations. The diffractive process represented by these oscillations would not likely survive unscathed the fuzzing caused by allowing the target to recoil. Nevertheless, the conditions producing the oscillations may persist (weak absorption, geometry) and they should perhaps be looked for experimentally in other reactions.

The absolute cross sections calculated for the $^{62,64}\text{Ni}$ reactions underestimate the measured cross sections by a factor ~ 3 .^{7,10} Those calculated for $^{58,60}\text{Ni}$ are down from measurement by perhaps 1.5. This change of normalization across the Ni isotopes may be associated with our use of a "no recoil" approximation or with inadequacies of our shell-model structure. Structure factors were taken from earlier theoretical studies¹¹ while the bound-state radius parameter and diffusivity were $r_0 = 1.25$ fm, $a = 0.65$ fm. Reasonable variations in bound-state parameters and in structure components produced no noticeable influence on angular distributions. It should be pointed out that attempts to shift normal bell-shaped angular distributions to more forward angles by increasing the radii of real and imaginary potentials is bound to fail. Not only will fits to elastic data be destroyed but, in addition, disturbingly low absolute cross sections are obtained for the reactions.

Strong transitions at angles forward of the expected grazing angle are also evident in measured angular distributions for the 57 and 65-MeV transitions to the 2^+ states in $^{60,62}\text{Ni}$ (Fig. 3). We expect a similar theoretical approach to that given above will adequately describe these reactions, but defer such an analysis to a later and more complete work.

In conclusion, several remarks seem relevant. The experimental differential cross sections for the $^{58,60}\text{Ni}(^{18}\text{O}, ^{16}\text{O})$ ground-state transitions showed marked deviations from cross sections expected in a grazing collision. A reasonable theoretical explanation is possible if the absorption is reduced considerably, probably only in the surface region of nuclear interaction. In the weaker absorbing environment the Q -value differences combine with radius changes (essentially dictated by elastic scattering fits) to produce the strong change in shape of the ($^{18}\text{O}, ^{16}\text{O}$) angular distributions across the Ni isotopes. In the calculations appreciable cross section is seen at extreme forward angles even for the $^{62,64}\text{Ni}$ targets. This point is being resolved by further

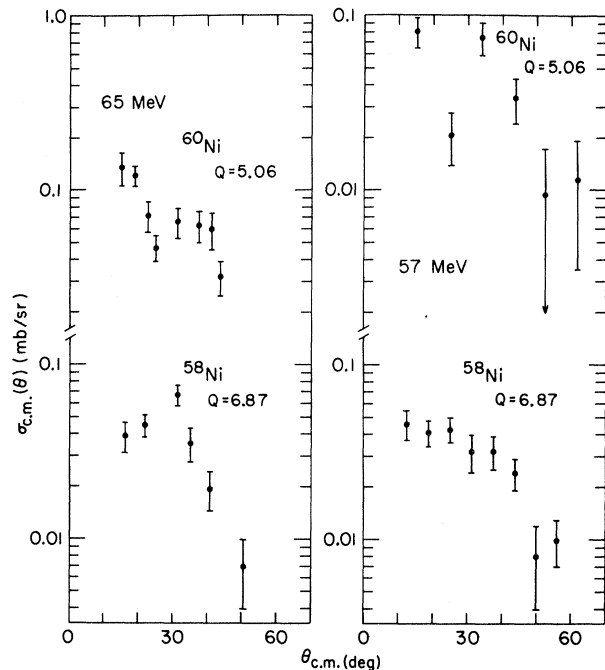


FIG. 3. Experimental differential cross sections for the $^{58,60}\text{Ni}(^{18}\text{O}, ^{16}\text{O})$ reactions to the first excited (2^+) states of $^{60,62}\text{Ni}$.

measurement. Other explanations for the changes seen may arise from more involved processes, such as multistep transfer. This remains for future work to explore. The change in optical potential throughout the Ni isotopes is not inconsistent with shell-model preconceptions for these nuclei, ^{64}Ni possessing considerably more valence neutrons than does ^{58}Ni . In any case the apparent sensitivity of the heavy-ion-induced transfer to optical parameters should prove useful in mapping out nucleus-nucleus interactions.

*Work performed under the auspices of the U. S. Atomic Energy Commission.

¹G. Breit and M. E. Ebel, Phys. Rev. **103**, 679 (1956); R. Broglia and A. Winther, Phys. Rep. **46**, No. 4 (1972).

²G. C. Morrison, J. Phys. (Paris), Colloq. C **6**, 69 (1971); H. Faraggi, M. C. Lemaire, J. M. Loiseau, M. C. Mermaz, and A. Papineau, Phys. Rev. C **4**, 1375 (1971); R. H. Siemssen, C. L. Fink, L. R. Greenwood, and H. J. Korner, Phys. Rev. Lett. **28**, 626 (1972); W. Von Oertzen, in "Nuclear Spectroscopy," edited by J. Cerny (Academic, New York, to be published).

³C. Chasman, S. Cochavi, M. J. LeVine, and A. Z. Schwarzschild, Phys. Rev. Lett. **28**, 843 (1972).

⁴F. Videbaek, J. Chernov, P. R. Christensen, and E. E. Gross, Phys. Rev. Lett. **38**, 1072 (1972); F. D. Becchetti, P. R. Christensen, V. J. Manko, and R. J. Nickles, in Proceedings of the International Conference

on Heavy Ion Physics, Dubna, 1971 (to be published).

⁵P. J. A. Buttle and L. J. B. Goldfarb, Nucl. Phys. **78**, 409 (1966).

⁶F. Schmittroth, W. Tobocman, and A. A. Golestaneh, Phys. Rev. C **1**, 377 (1970).

⁷A. J. Baltz and S. Kahana, Phys. Rev. Lett. **29**, 1267 (1972).

⁸M. C. Bertin, Y. Eisen, G. Goldring, S. L. Tabor, and B. A. Watson, Nucl. Phys. **A167**, 216 (1971).

⁹R. M. DeVries and K. I. Kubo, Phys. Rev. Lett. **30**, 325 (1973).

¹⁰B. F. Bayman, Phys. Rev. Lett. **25**, 1768 (1970).

¹¹L. S. Kisslinger and R. A. Sorensen, Kgl. Dan. Vidensk. Selsk., Mat.-Fys. Medd. **32**, No. 9 (1960).

Rapidly Rotating Neutron Stars*

James R. Wilson

Lawrence Livermore Laboratory, University of California, Livermore, California 94550

(Received 20 February 1973)

Models of differentially rotating neutron stars have been calculated. An upper limit to the rotational enhancement of the maximum gravitational mass is found to be about 50% when the Ostriker-Tassoul instability criterion is used.

The search for black holes depends, to a large extent, on finding compact stars whose masses exceed the accepted maximum mass for a neutron star. Hartle and Thorne¹ have calculated the increase in mass to be expected in a rigidly rotating neutron star. The object of the present work is to relax the condition of uniform rotation and see if the mass of a neutron star can be increased significantly.

In the present work, sequences of increasingly faster-rotating, axially symmetric equilibrium configurations are found for a given equation of state, using the fully relativistic equations. In order to terminate the sequences, the Ostriker-Tassoul² stability criterion is used.

The notation used here and the equations for the metric and hydrostatic equilibrium are taken from Bardeen and Wagoner³ and Wilson.⁴ The method of solution is different and is as follows. An estimate of density versus radius of a neutron star is assumed, and the field equations are solved for the metric. Next, the Z component of Eq. (5) from Ref. 4 is solved for density by integrating out from the equator. The boundary condition on the integration is that the mass per unit coordinate volume on the equator is fixed. Then the R component of Eq. (5) is solved for the angular velocity. Using the new densities and velocities, the field equations are solved again for the metric. Then the hydrostatic equation is again solved for the new densities and velocities. This alternation back and forth between field equations and equilibrium equations is repeated until a convergence is achieved. Thus, a nearly spherical configuration is first established. To find more rapidly rotating models, the density

profile in the equator is simply stretched out in the R direction in proportion to the radius, and the above iteration procedure is carried through again.

Since the equations are solved by finite-difference methods by a rather small number of grid points (about 25×25), coarse (15×15) and fine-zoned (25×25) problems were run on two of the configurations. From this, the error in mass is estimated to be probably less than 5%. The Tolman-Oppenheimer-Volkoff equation was integrated in a fine grid, using the same equation of state. The mass of the spherical stars, as calculated with the two-dimensional program, agreed within better than 5% with the accurate spherical calculation.

Wilson's⁵ equation of state III was used except where indicated. This equation of state yields a maximum gravitational mass of $1.90M_{\odot}$, and so it is probably as hard an equation of state as is now popular. Star configurations with three different central densities were calculated with the above equation of state. Due to the calculational procedure used, the central density decreases as the rotation increases in a sequence with increasing rotation. Figure 1 gives the star masses and central densities for the three calculations.

Ostriker and Tassoul² found that rotating, gravitationally bound systems have nonaxially symmetric modes of instability, independent of the degree of differential rotation. The density distributions for the examples with high central density (B and C of Fig. 1) are relatively flat. The isodensity contour $\frac{2}{10}$ of the way in from the outside of the star indicates a density $\frac{1}{10}$ that of the central density. We infer from this that the lin-